values seem to show too a high scatter so that an independence of the ligand basicity cannot be assumed. In particular the data show a tendency to enhanced reactivity with decreasing the strength of the carboxylic group of the ligands, i.e., the basicity of their conjugated base; therefore our results provide additional evidence that a departure from a dissociative behavior is present for Fe^{3+} ion.[3,9,10]

Registry No. Fe, 7439-89-6; Cl(SAL), 321-14-2; N(SAL), 96-97-9; OH(SAL), 303-07-1; DN(SAL), 609-99-4; SAL, 69-72-7; SSAL, 97-05-2; PAS, 65-49-6.

Contribution from Anorganische Chemie III,
Eduard-Zintl-Institut der Technischen Hochschule Darmstadt, D-6100 Darmstadt, Federal Republic of Germany

Steric and Conformational Effects on the Kinetics of Ligand Substitution in Bis(salicylaldiminato)nickel(II) Complexes

MANFRED SCHUMANN, ANGELA von HOLTUM, KLAUS J. WANNOWIUS, and HORST ELIAS*

Received March 10, 1981

Stopped-flow spectrophotometry has been used to study the kinetics of ligand substitution in bis(*N*-R-salicylaldiminato)nickel(II) complexes I (R = Et, *i*-Pr, *t*-Bu) by bidentate ligands HB (acetylacetone, benzoylacetone, dibenzoylmethane, trifluoroacetylacetone, 8-hydroxyquinoline, *N*-ethylsalicylaldimine) in methanol, 2-propanol, and toluene. A two-term rate law, rate = $(k_S + k_{HB}[HB])$[complex], has been found. The substitution of the first ligand in I is rate determining. Rate constant k_S, describing the solvent path, and the corresponding activation parameters $\Delta H^{\ddagger}$ and $\Delta S^{\ddagger}$ do not depend on the nature of the entering ligand for I with R = *t*-Bu studied in methanol. Rate constant k_{HB} is strongly dependent on the nature of the entering ligand HB. The relative contributions of the two pathways to the overall rate are governed by the conformational equilibrium planar $\rightleftharpoons$ tetrahedral of complexes I: the planar isomer favors the ligand-dependent path k_{HB} and the tetrahedral one the solvent path k_S. For both pathways mechanisms are derived, which have in common the rate-determining rupture of the Ni–O bond. They differ in that the solvent path is initiated by the attack of an alcohol molecule at the donor oxygen of a coordinated ligand through hydrogen bonding, whereas ligand attack occurs at the metal. The factors influencing the ligand path are the donor ability, acid strength, and stereochemical properties of the entering ligand as well as the Lewis acidity of the substrate. The discussion focuses on a comparison of the nickel system studied with corresponding copper(II) systems and with ligand substitution in square-planar d^8 complexes. Additional kinetic information is presented from studies carried out in the solvent mixtures toluene/methanol and toluene/pyridine. The equilibrium constant for the addition of pyridine to complexes I (R = Et, *n*-Pr, *i*-Pr, allyl, *n*-Bu, *i*-Bu, *t*-Bu, phenyl) has been determined spectrophotometrically in toluene at 298 K. The individual equilibrium constants for the formation of the mono- (K_1) and bis(pyridine) (K_2) adduct were calculated ($K_1 << K_2$). The effect of the conformational equilibrium and of self-association on K_1 and K_2 is discussed.

Introduction

The kinetics of ligand substitution in square-planar platinum(II) and palladium(II) complexes according to

$$ML_3X + Y \rightleftharpoons ML_3Y + X$$

appears to be a matter well understood.[1] There is general agreement that the mechanism of substitution is associative in character for both the solvent path k_S and the reagent path $k_Y[Y]$, forming the observed rate law

$$k_{obsd} = k_S + k_Y[Y]$$

It is generally assumed that this is also true for other d^8 systems although there is much less experimental evidence for metal centers such as Ni(II), Ir(I), or Au(III).

As pointed out by Billo[2] and recently by Fayyaz and Grant,[3] in the case of nickel(II) the choice of suitable square-planar complexes is strongly restricted. As a consequence, the relatively few kinetic studies on ligand substitution in planar nickel(II) complexes have been concerned with S_4 and N_4 chelate complexes of types A–C. The kinetics of ligand substitution in bis(dithiolato) complexes of type A[4] and in type B complexes[2] were studied in aqueous solution, bidentate or monodentate nucleophiles serving as entering ligands. Studies

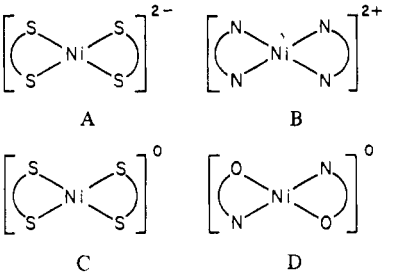

with neutral bis(dithiophosphato) and bis(dithiocarbamato) complexes of type C were carried out in methanol[5] and acetone.[3] The ligand substitution in complexes A, B, and C proceeds exclusively through a reagent path, clearly associative in character. So, in contrast to the intensely studied Pt(II) substrates these complexes seem not to allow a solvent pathway.

In this paper we present further information on the kinetic behavior of neutral four-coordinate nickel(II) bis-chelate species in chelate ligand substitution reactions carried out in organic media. In contrast to the neutral S_4 complexes of type C the complexes studied here are of the *trans*-N_2O_2 type D with *N*-alkylsalicylaldimines (≡HSA═*N*-R) serving as ligands.

The X-ray structures of the complexes Ib and Ic have been determined. Ic exhibits a coordination geometry that is essentially planar (so-called stepped structure[6b]). In Ib the

(1) Basolo, F.; Pearson, R. G. "Mechanisms of Inorganic Reactions", 2nd ed.; Wiley: New York, 1967; Chapter 5.
(2) Billo, E. J. *Inorg. Chem.* **1973**, *12*, 2783.
(3) Fayyaz, M. U.; Grant, M. W. *Aust. J. Chem.* **1979**, *32*, 2159.
(4) Pearson, R. G.; Sweigart, D. A. *Inorg. Chem.* **1970**, *9*, 1167.
(5) Hynes, M. J.; Brannick, P. F. *J. Chem. Soc., Dalton Trans.* **1977**, *2281*.

0020-1669/82/1321-0606$01.25/0

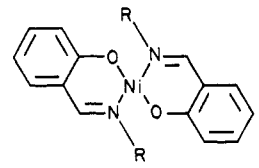

I ≡ NiA_2 ≡ Ni(SA=*N*-R)$_2$
Ia (R = *t*-Bu) ≡ Ni(SA=*N*-*t*-Bu)$_2$
b (R = *i*-Pr) ≡ Ni(SA=*N*-*i*-Pr)$_2$
c (R = Et) ≡ Ni(SA=*N*-Et)$_2$

nickel is almost tetrahedrally surrounded by the donor atoms (the dihedral angle formed by the planes of the two chelate ligands is Θ = 81.5°[6b]). Although there is no X-ray structure of Ia, one can conclude from the corresponding copper(II) complex,[6b] from reflectance spectra,[7] and also from magnetic data[7] that this complex is pseudotetrahedral in the solid state.

In solution the coordination geometry of the bis(salicylaldiminato)nickel(II) complexes is characterized by the two equilibria

$$\text{octahedral} \overset{K_{o,p}}{\rightleftharpoons} \text{planar} \overset{K_{p,t}}{\rightleftharpoons} \text{tetrahedral} \quad (1a,b)$$

Bulky R groups such as *tert*-butyl do not allow the formation of square-planar and octahedral species ($K_{p,t} >> 1$). For R = isopropyl the equilibria are considerably shifted to the left. For complexes with straight-chain or β-C-branched alkyl R groups equilibrium 1a becomes dominating ($K_{p,t} << 1$). In solvents with good donor properties such as pyridine and MeOH two solvent molecules are coordinated in the axial positions and hexacoordination is achieved. In many cases bisadducts such as [Ni(SA=*N*-R)$_2$(py)$_2$][8] or [Ni(SA=*N*-*i*-Pr)$_2$(MeOH)$_2$][9] have been isolated. In the absence of donor molecules self-association becomes the major process leading to the formation of paramagnetic hexacoordinated oligomers.

The reaction studied is described by (2) with NiA_2 ≡ Ia–c

$$NiA_2 + 2HB \rightleftharpoons NiB_2 + 2HA \quad (2)$$

and HB ≡ acetylacetone (Hacac), benzoylacetone (Hbza), dibenzoylmethane (Hdbm), trifluoroacetylacetone (Htfa), 8-hydroxyquinoline (Hox), or *N*-ethylsalicylaldimine (HSA=*N*-Et). The solvents applied are methanol (MeOH), 2-propanol (2-PrOH), and toluene.

In addition to these kinetic studies the Lewis acidity of various complexes I (R = Et, *n*-Pr, *i*-Pr, *n*-Bu, *i*-Bu, *t*-Bu, allyl, phenyl) toward pyridine is characterized by the determination of *K* in toluene:

$$NiA_2 + 2py \rightleftharpoons NiA_2(py)_2 \quad K \quad (3)$$

The contribution aims at a correlation of the data for equilibria 1 and 3 with the kinetic data for reaction 2 in order to attack the question of how reactive a planar nickel(II) complex I is relative to its tetrahedral conformational isomer.

Experimental Section

Complexes and Ligands. The various complexes I were prepared by the following standard procedure. A 0.04-mol quantity of bis(salicylaldehydato)nickel(II) dihydrate (which precipitates from a solution of $Ni(AcO)_2 \cdot 6H_2O$ in EtOH/H_2O (1:1) upon addition of salicylaldehyde[10]) and 0.1 mol of the appropriate amine in 100 mL of MeOH were refluxed until the solid had dissolved. After evaporation of the solvent in vacuo the dark-colored solid residue was recrystallized from ethyl acetate, yielding a very pure crystalline product (yield 50–80%). Since the complex Ni(SA=*N*-*t*-Bu)$_2$ is easily hydrolyzed, it had to be recrystallized from dried ethyl acetate in a dry atmosphere. The results of elemental analysis agreed well with calculated data, and the melting points of the complexes were those reported in the literature.[11]

N-Ethylsalicylaldimine was prepared as described earlier.[12] Acetylacetone and trifluoroacetylacetone (reagent grade, Merck, Darmstadt) were distilled before use (bp 136 and 106 °C) whereas benzoylacetone and dibenzoylmethane were recrystallized from MeOH. 8-Hydroxyquinoline (reagent grade, Merck, Darmstadt) was used without further purification.

Solvents. MeOH, 2-PrOH, and toluene (all reagent grade, Merck, Darmstadt) were dried dynamically over 3- or 4-Å molecular sieves. The residual water content was 10^{-3} to 5×10^{-3} M as determined by automatic Karl Fischer titration.

Kinetic Measurements. The kinetic measurements were done with a modified[12] Durrum D110 stopped-flow spectrophotometer in combination with an Aminco DASAR storage oscilloscope. The kinetic runs were done under pseudo-first-order conditions ([ligand] ≥ 20[complex]) and monitored at 545–700 nm. Reproducible runs were evaluated by fitting a total of 200 data points to an exponential function with a computer program based on the least-squares method. The deviation from ideal first-order kinetics was smaller than 1%.

Equilibrium Constants. For the determination of the equilibrium constants *K* solutions of the various complexes I in toluene were titrated stepwise with pyridine (15–20 steps) and the spectra recorded with a Zeiss DMR 22 spectrophotometer. The calculation of *K* was based on the decrease in the absorbance *A* at 620 nm upon addition of pyridine. The data were fitted to eq 4 and 5 with computer programs described earlier.[13] Equation 4 can easily be derived from the overall

$$A = \{A^\circ(NiA_2) + K(A^\circ(NiA_2(py)_2))[py]^2\}/\{1 + K[py]^2\} \quad (4)$$

$$A = \{A^\circ(NiA_2) + (A^\circ(NiA_2py))K_1[py] + (A^\circ(NiA_2(py)_2))K_1K_2[py]^2\}/\{1 + K_1[py] + K_1K_2[py]^2\} \quad (5)$$

equilibrium (3). Similarly eq 5 is obtained when the formation of a 5-coordinate intermediate is allowed (eq 6). The symbols $A^\circ(NiA_2)$,

$$\begin{aligned} NiA_2 + py &\rightleftharpoons NiA_2py \quad K_1 \\ NiA_2py + py &\rightleftharpoons NiA_2(py)_2 \quad K_2 \end{aligned} \quad (6)$$

Table I. Equilibrium Constants for Adduct Formation of the Complexes I with Pyridine in Toluene at 298 K[a]

R	K,[b] M^{-2}	K_1,[c] M^{-1}	K_2,[c] M^{-1}	$\beta = K_1K_2$, M^{-2}	K,[d] M^{-2}
Et	141 ± 4	3.0	52	155	
n-Pr	146 ± 3	2.5	61	153	100 ± 15
i-Pr	314 ± 4	3.0	83	259	150 ± 25
allyl	199 ± 4	3.0	55	163	
n-Bu	164 ± 4	2.0	77	153	130 ± 30, 282 ± 80[e]
i-Bu	176 ± 4	2.4	71	169	
t-Bu	≤0.1[f]				
Ph[g]	975 ± 96				1000 ± 200
Et[h]		0.54[h]			
i-Pr[h]		0.21[h]			
t-Bu[h]		0.31[h]			
Ph[h]		1.75[h]			

[a] $[Ni]_{tot} = 5 \times 10^{-3}$ M. [b] Determined by computer fitting to eq 4. [c] Determined by computer fitting to eq 5. [d] For benzene solution at 303 K from ref 14a. [e] For benzene solution at 298 K from ref 14b; $K_1 = 3.1\ M^{-1}$, $K_2 = 91\ M^{-1}$. [f] Approximated; the value is not very reliable due to incomplete formation of the bisadduct. [g] $[Ni]_{tot} = 2 \times 10^{-3}$ M. [h] *K* for the formation of the corresponding monoadducts Cu(SA=*N*-R)$_2$(py) from ref 13b.

(6) (a) Holm, R. H.; Everett, G. W., Jr.; Chakravorty, A. *Prog. Inorg. Chem.* **1966**, *7*, 83. (b) Holm, R. H.; O'Connor, M. J. *Ibid.* **1971**, *14*, 241.
(7) Sacconi, L.; Ciampolini, M.; Nardi, N. *J. Am. Chem. Soc.* **1964**, *86*, 819.
(8) See, for example: (a) Basolo, F.; Matoush, W. R. *J. Am. Chem. Soc.* **1953**, *75*, 5663. (b) Clark, H. C.; Odell, A. L. *J. Chem. Soc.* **1955**, 3431.
(9) Sacconi, L.; Ciampolini, M. *J. Am. Chem. Soc.* **1963**, *85*, 1750.
(10) Tyson, G. N.; Adams, S. C. *J. Am. Chem. Soc.* **1940**, *62*, 1228.
(11) "Gmelins Handbuch der Anorganischen Chemie"; Verlag Chemie: Weinheim, Germany; System No. 57, Nickel, Part C[2].
(12) Elias, H.; Fröhn, U.; Irmer, A. v.; Wannowius, K. J. *Inorg. Chem.* **1980**, *19*, 869.
(13) (a) Reiffer, U.; Schumann, M.; Wannowius, K. J.; Elias, H. *Transition Met. Chem.* **1980**, *5*, 272. (b) Ewert, A.; Wannowius, K. J.; Elias, H. *Inorg. Chem.* **1978**, *17*, 1691.

$A°(NiA_2py)$ and $A°(NiA_2(py)_2)$ in (4) and (5) refer to the absorbance of the species NiA_2, NiA_2py and $NiA_2(py)_2$ at a concentration of $[Ni]_{tot}$. The concentration [py] in (4) and (5) can be replaced by $[py]_{tot}$ as long as the condition $[py]_{tot} >> [Ni]_{tot}$ is fulfilled.

Results and Discussion

Acceptor Properties of the Complexes in Solution. The kinetic studies of this contribution were carried out in different solvents. It is obvious that any mechanistic discussion of the observed reaction pathways should include the state of solvation and conformation of the complexes according to (1a) and (1b). The addition of nucleophiles such as pyridine can be taken as a meaningful model reaction for the solvation by polar solvent molecules. Therefore, the acceptor properties of various complexes I toward pyridine were studied first.

A proof for bisadduct formation according to (3) can be derived from a plot of the parameter $\log [(A - A°(NiA_2))/(A°(NiA_2(py)_2) - A)]$ vs. $\log [py]$ (see eq 4). Such a plot led indeed to the expected straight lines, which in all cases had a slope of approximately 2. The overall equilibrium constant K can be obtained on the basis of relationship 4. The computer fitting of the absorbance data with (4) (i.e., without consideration of a 5-coordinate intermediate) leads to the K values listed in Table I. The standard deviation of the fit is further reduced, however, when the formation of the monoadduct according to (5) and (6) is considered. In this way the individual equilibrium constants K_1 and K_2 of Table I were obtained.

The most striking finding is that $K_1 << K_2$. The tendency of the complexes to form the 6-coordinate bis(pyridine) adduct is so strong that the proportion of the intermediate monoadduct is small and never exceeds 10% of $[Ni]_{tot}$. Another interesting result is a very close similarity between the K and β values in Table I. Hence, the formation of the bisadducts can fairly well be approximated by the one-step process (3).

The K values derived in this work parallel convincingly those determined calorimetrically by Dakternieks and Graddon[14a] in benzene solution (see Table I). Since the addition of pyridine is an exothermic process, the cited data, obtained at 30 °C, are somewhat lower. The data reported in the literature[14b] for K_1 and K_2 of the complex $Ni(SA{=}N\text{-}n\text{-}Bu)_2$ in benzene solution are slightly higher ($K_1 = 3.1\ M^{-1}$; $K_2 = 91\ M^{-1}$; $\beta = K_1K_2 = 282 \pm 80\ M^{-2}$). One has to take into account, however, that they were determined with a relatively large error.

On the basis of (1) the complexes listed in Table I can be classified according to the position of the equilibrium planar $\rightleftharpoons$ tetrahedral (1b): $K_{p,t}$ is estimated to be very large for Ia ($K_{p,t} >> 1$), close to unity for Ib, and very small for all the other complexes I with aliphatic groups R ($K_{p,t} << 1$). For Ia the spectral changes observed upon addition of pyridine are very small and the determination of the equilibrium constant is not very reliable; therefore $K \leq 0.1\ M^{-2}$. The similarity of the K_2 values given in Table I seems to support the assumption that K_2 is rather insensitive to the nature of R.

With regard to the significance of the K_1 values one has to consider that in toluene complexes I exist as tetrahedral or square-planar monomeric species and as self-associated oligomers. It is assumed that the addition of pyridine occurs through the square-planar form only, as shown in Scheme I. On the basis of this scheme the experimentally determined constant K_1 is related to K_{as} (self-association), $K_{p,t}$, and K_1':

$$K_1 = \frac{K_1'}{1 + K_{p,t} + nK_{as}[(NiA_2)_p]^{n-1}} \qquad (7)$$

Scheme I. Stereochemical Equilibria in the Presence of Pyridine

$$(1/n)(NiA_2)_n \overset{K_{as}^{-1}}{\rightleftharpoons} (NiA_2)_c \overset{K_{p,t}}{\rightleftharpoons} (NiA_2)_p$$
$$\Big\| K_1' \qquad\qquad\qquad\qquad \Big\| K_1'$$
$$[NiA_2py] \qquad\qquad\qquad\qquad [NiA_2py]$$
$$\Big\| K_2$$
$$[NiA_2(py)_2]$$

Equation 7 clearly demonstrates that either high $K_{p,t}$ values and/or high K_{as} values reduce K_1.

For some of the complexes I the degree of self-association has been measured in toluene and xylene.[15] The equilibrium constants for dimer formation can be estimated to be $K_{as} = [dimer]/[monomer]^2 \approx 400\ M^{-1}$ (for R = Ph; a value of $K_{as} \approx 2000\ M^{-1}$ can be roughly estimated from ref 9 for 25 °C) and $K_{as} \approx 1\ M^{-1}$ (for R = *i*-Pr and R = Me) at 37 °C. The contribution of K_{as} to the denominator in (7) is significant only for the phenyl complex ($2K_{as}[(NiA_2)_p] > 1$ at $[Ni]_{tot} = 2 \times 10^{-3}$ M). The strong self-association is responsible for the ratio K_1/K_2 to be so small that computer fitting of the data does not produce meaningful K_1 values for this complex. Due to the electron-withdrawing effect of the phenyl groups the K value is large, however, which parallels the trend observed for the analogous copper complexes (see Table I).

The only complex in Table I for which $K_{p,t}$ contributes significantly to K_1 is Ia (R = *t*-Bu). As a result the equilibrium constant is strongly reduced. For the complexes I with R = Et, *n*-Pr, *i*-Pr, *n*-Bu, *i*-Bu, and allyl, K_1 nearly equals K_1'. The constant K_1 values (see Table I) within this group of complexes demonstrate this convincingly.

One basic difference between adduct formation of $Ni(SA{=}N\text{-}R)_2$ and $Cu(SA{=}N\text{-}R)_2$ is that the copper complexes form monoadducts only and the nickel complexes form most stable bisadducts. A comparison of the corresponding K_1 values for R = Et and R = *i*-Pr demonstrates however (see Table I) that even the monoadduct is more stable with nickel than with copper (surprisingly, this is not so for R = *t*-Bu).

The rate of pyridine addition is comparatively high. The adduct formation of $Ni(SA{=}N\text{-}n\text{-}Bu)_2$ and of $Ni(SA{=}N\text{-}Ph)_2$ with pyridine was too fast to be detected by the stopped-flow technique.

In combination with information obtained from the UV/vis absorption spectra the equilibrium studies described above are pertinent to the kinetic studies in the sense that they allow predictions on the state of solvation and conformation of complexes Ia–c in the various solvents. In toluene the complexes Ia–c will be mainly monomeric. For Ib and even more so for Ic, however, self-associated oligomers will be present. In the series Ia << Ib < Ic the fraction of the square-planar form increases. The same is true for MeOH and 2-PrOH solutions, but 6-coordinate adducts with the solvent are more likely than oligomers. The reported isolation of $Ni(SA{=}N\text{-}i\text{-}Pr)_2(MeOH)_2$[9] can be taken as additional proof. Spectral changes in the charge-transfer range of the spectra in going from toluene to MeOH or 2-PrOH solutions point to some additional interaction (probably hydrogen bonding as typical for protic solvents). This effect will be discussed later.

Kinetic Results. It is obvious that the reaction $NiA_2 \rightarrow NiB_2$ according to (2) has to take place stepwise:

$$NiA_2 \xrightarrow[+HB,\ -HA]{\text{step 1}} NiAB \xrightarrow[+HB,\ -HA]{\text{step 2}} NiB_2 \qquad (8)$$

As described previously[12,16] for ligand substitution in various

(14) (a) Dakternieks, D. R.; Graddon, D. P. *Aust. J. Chem.* **1973**, *26*, 2379. (b) Dakternieks, D. R.; Graddon, D. P.; Lindoy, L. F.; Mockler, G. M. *Inorg. Chim. Acta* **1973**, *7*, 467.

(15) (a) Holm, R. H.; Swaminathan, K. *Inorg. Chem.* **1962**, *1*, 599. (b) *Ibid.* **1963**, *2*, 181.

Table II. Rate Constants for the First Step of Reaction 8 at 298 K

system	complex	entering ligand	solvent	k_S, s^{-1}	k_{HB}, $M^{-1} s^{-1}$
1	Ni(SA=*N*-*t*-Bu)$_2$	Hox	MeOH	1.13 ± 1.3	259 ± 8
2	Ni(SA=*N*-*t*-Bu)$_2$[a]	Htfa[a]	MeOH	0.88 ± 0.19	76.7 ± 2.8
3	Ni(SA=*N*-*t*-Bu)$_2$	Hdbm	MeOH	0.86 ± 0.02	2.33 ± 0.54
4	Ni(SA=*N*-*t*-Bu)$_2$	Hbza	MeOH	0.86 ± 0.04	1.14 ± 0.13
5	Ni(SA=*N*-*t*-Bu)$_2$	Hacac	MeOH	0.90 ± 0.01	0.52 ± 0.02
6	Ni(SA=*N*-*t*-Bu)$_2$	HSA=*N*-Et	MeOH	0.88 ± 0.01	<0.1
7	Ni(SA=*N*-*i*-Pr)$_2$	HSA=*N*-Et	MeOH	0.39 ± 0.2	69.6 ± 1[b]
8	Ni(5-MeSA=*N*-Et)$_2$[c]	HSA=*N*-Et	MeOH	1 ± 1.6	65.5 ± 5.9
9	Ni(SA=*N*-*i*-Pr)$_2$	Hacac	MeOH	<5	1470 ± 38
10	Ni(SA=*N*-Et)$_2$	Hacac	MeOH	<5	2070 ± 37
11	Ni(SA=*N*-*t*-Bu)$_2$	HSA=*N*-Et	2-PrOH	0.0038 ± 0.0001	0.0092 ± 0.0001
12	Ni(SA=*N*-*i*-Pr)$_2$	HSA=*N*-Et	2-PrOH	<0.5	51.8 ± 1
13	Ni(SA=*N*-*t*-Bu)$_2$	HSA=*N*-Et	toluene	[e]	0.031 ± 0.002
14	Ni(SA=*N*-*i*-Pr)$_2$	HSA=*N*-Et	toluene	[e]	11.5 ± 0.5
15	Cu(SA=*N*-*t*-Bu)$_2$[d]	HSA=*N*-Et	MeOH	0.95 ± 0.04[d]	<0.1[d]
16	Cu(SA=*N*-*i*-Pr)$_2$[d]	HSA=*N*-Et	MeOH	0.10 ± 0.009[d]	<0.01[d]
17	Cu(5-MeSA=*N*-Et)$_2$[c,d]	HSA=*N*-Et	MeOH	0.012 ± 0.001[d]	0.0056 ± 0.0006[d]

[a] Data for the second step of reaction 8: $k_S < 0.5$ s^{-1}; $k_{HB} = 29.4 \pm 9.0$ M^{-1} s^{-1}. [b] $\Delta H^{\ddagger}(k_{HB}) = 34.0 \pm 1.1$ kJ mol^{-1}; $\Delta S^{\ddagger}(k_{HB}) = -95.6 \pm 3.5$ J mol^{-1} K^{-1}. [c] Complex derived from *N*-ethyl-5-methylsalicylaldimine. [d] Data from ref 22. [e] Not observed.

copper complexes Cu(SA=*N*-R)$_2$, it was also found for the majority of the nickel substitution reactions studied in this work that the first step of sequence 8 is the slow and rate-controlling one, the second being a fast consecutive reaction. This assignment is based on three experimental facts: (i) the spectrometric signal observed corresponds to pure Ia, Ib, or Ic at $t = 0$ and to pure product NiB_2 at $t = \infty$; (ii) the change in absorbance with the time can be fitted to a single exponential function with an accuracy > 99%; (iii) for a given complex NiA_2 the size of k_S (see eq 9) does not depend on the nature of the entering ligand, which it should if step 2 were observed.

The only exception found was the reaction of Ni(SA=*N*-*t*-Bu)$_2$ in MeOH with Htfa as the incoming ligand. Here the time dependence of the absorbance A is more adequately represented by the function $A = a \exp(-k_a t) + b \exp(-k_b t) + c$. The assignment of the observed rate constants k_a and k_b to the first and second steps of (8), respectively, was possible on the basis of the values obtained for the extinction coefficient ϵ(NiAB) of the intermediate after computer fitting of the data (one of the two mathematical solutions produces a negative ϵ(NiAB), which is chemically meaningless).

The dependence of the pseudo-first-order rate constant k_{obsd} on the concentration of the entering ligand HB was measured at $[NiA_2] = 0.002$ M in the range [HB] = 0.02–0.5 M. In all systems studied the rate follows eq 9. It is important to

$$\text{rate} = k_{obsd}[NiA_2] = (k_S + k_{HB}[HB])[NiA_2] \quad (9)$$

note that in some systems the ligand-independent "solvent path" k_S dominates ($k_S >> k_{HB}[HB]$), and in others the ligand-dependent "reagent path" or "ligand path" dominates ($k_{HB}[HB] >> k_S$). Figure 1 presents one example for each of the different types of ligand dependence observed. The data obtained for k_S and k_{HB} are summarized in Table II; they refer to the first step of (8), i.e., to the reaction $NiA_2 \rightarrow NiAB$.

The solvent-initiated pathway k_S of ligand substitution in square-planar platinum(II) complexes is independent of the nature of the incoming ligand.[1] Although having a tetrahedral coordination geometry complex, Ia also displays this type of behavior. In MeOH as solvent the values obtained for k_S are constant for a variety of entering ligands (see systems 1–6 in Table II). Figure 2 presents convincing proof for this and for the quality of the experimental data obtained in the β-diketone systems 2–5 (since k_S is determined by extrapolation to [HB] = 0, the limits of error grow with increasing size of k_{HB}, as demonstrated by system 1). In the case of Hbza and Hdbm

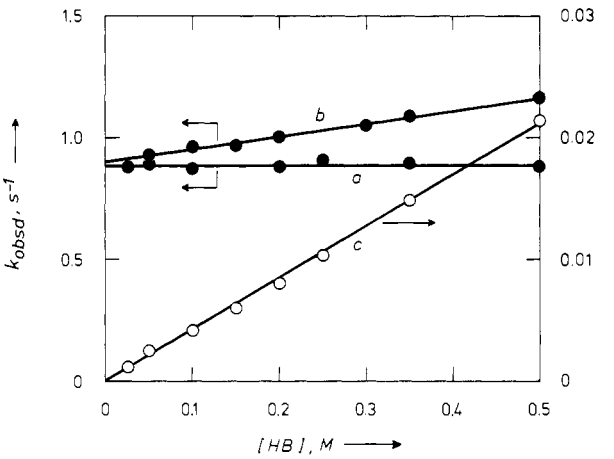

Figure 1. Dependence of k_{obsd} on the ligand concentration for ligand substitution in Ni(SA=*N*-*t*-Bu)$_2$ at 298 K ([Ni(SA=*N*-*t*-Bu)$_2$] = 2×10^{-3} M): curve a, HB ≡ HSA=*N*-Et in MeOH; curve b, HB ≡ Hacac in MeOH; curve c, HB ≡ HSA=*N*-Et in toluene.

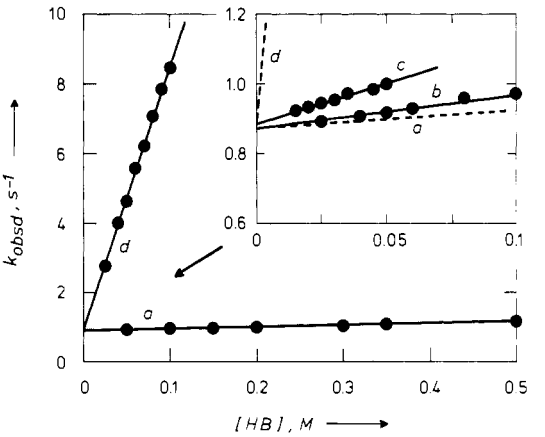

Figure 2. Ligand substitution in Ni(SA=*N*-*t*-Bu)$_2$ by various β-diketones at 298 K in MeOH ([Ni(SA=*N*-*t*-Bu)$_2$] = (1.0–2.0) × 10^{-3} M): curve a, HB ≡ Hacac; curve b, HB ≡ Hbza; curve c, HB ≡ Hdbm; curve d, HB ≡ Htfa.

the concentration range covered is limited by solubility. The ligand independence of k_S is further supported by the fact that the activation parameters $\Delta H^{\ddagger}$ and $\Delta S^{\ddagger}$ as derived from the temperature dependence of k_S are remarkably constant for the systems 3–6 (see Table III).

Figure 3 demonstrates the effect brought about by additional free leaving ligand in systems 6 and 7. Increasing amounts

(16) Elias, H.; Reiffer, U.; Schumann, M.; Wannowius, K. J. *Inorg. Chim. Acta* **1981**, *53*, L65.

Table III. Activation Parameters for the Solvent Path As Determined in Methanol[a]

complex	entering ligand	$\Delta H^{\ddagger}$, kJ mol^{-1}	$\Delta S^{\ddagger}$, J mol^{-1} K^{-1}
Ni(SA=*N*-*t*-Bu)$_2$	Hdbm	38.5 ± 1.3	−116.6 ± 4.2
Ni(SA=*N*-*t*-Bu)$_2$	Hbza	38.1 ± 0.5	−118.3 ± 1.7
Ni(SA=*N*-*t*-Bu)$_2$	Hacac	38.0 ± 0.7	−118.2 ± 2.1
Ni(SA=*N*-*t*-Bu)$_2$	HSA=*N*-Et	38.9 ± 0.8	−115.8 ± 2.6
Cu(SA=*N*-*t*-Bu)$_2$[b]	HSA=*N*-Et	60.7 ± 0.5[b]	−41.8 ± 1.6[b]

[a] Determined from the temperature dependence of k_S for the first step of reaction 8 at 5 or 6 temperatures in the range 20-50 °C. [b] Data from ref 12.

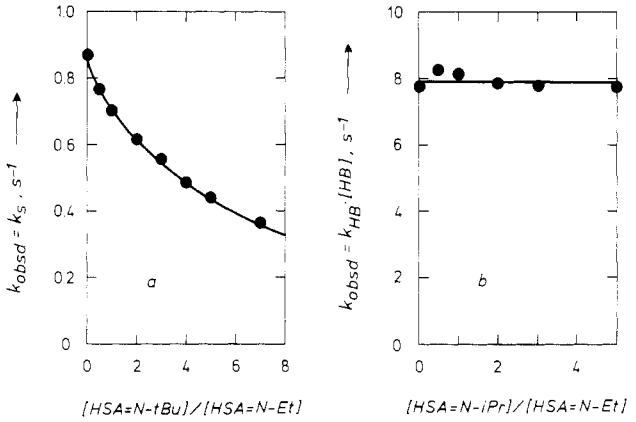

Figure 3. Effect of additional leaving ligand on k_{obsd} for ligand substitution in (a) Ni(SA=*N*-*t*-Bu)$_2$ and (b) Ni(SA=*N*-*i*-Pr)$_2$ by HSA=*N*-Et in MeOH at 298 K ([complex] = 2 × 10^{-3} M).

of HSA=*N*-*t*-Bu clearly reduce the rate of the solvent-induced ligand substitution in Ni(SA=*N*-*t*-Bu)$_2$ (see Figure 3a) whereas for the complex Ni(SA=*N*-*i*-Pr)$_2$ the value obtained for k_{HB} does not change upon addition of HSA=*N*-*i*-Pr (see Figure 3b). So, as in the case of the corresponding copper complexes,[16] there is a mass law retardation for the solvent path but not for the ligand path.

As shown in Figure 1 ligand substitution in Ni(SA=*N*-*t*-Bu)$_2$ by HSA=*N*-Et does occur exclusively through the solvent path in MeOH. It is to be expected therefore that the addition of MeOH to toluene introduces a very efficient solvent path. Figure 4 presents the dependence of k_S on the concentration of MeOH in toluene (already at [MeOH] ≥ 0.6 M the contribution of the ligand path to the observed rate constant becomes negligible). As one can see, there is a linear dependence of k_S on [MeOH] up to [MeOH] ≤ 1 M. At higher concentrations of MeOH the increase in k_S with increasing concentration of MeOH is also linear; the slope, however, becomes smaller (k_S was determined up to [MeOH] = 24.6 M, which corresponds to pure MeOH).

As pointed out earlier the complex Ni(SA=*N*-*i*-Pr)$_2$ forms a rather stable bisadduct with pyridine (β = 259 M^{-2}; see Table I). In a preliminary study the rate for the first step of ligand substitution in Ni(SA=*N*-*i*-Pr)$_2$ by HSA=*N*-Et was measured in toluene in the presence of 1 M pyridine (at this concentration >99% of the total nickel is present as [Ni(SA=*N*-*i*-Pr)$_2$(py)$_2$]). The rate constants for the solvent and the ligand path are k_S = 1.9 s^{-1} and k_{HB} = 1.1 M^{-1} s^{-1}. As compared to the addition of pure toluene as solvent (system 14 in Table II) the addition of pyridine clearly opens a ligand-independent reaction channel and simultaneously reduces the size of the ligand path.

Mechanism of the Ligand Path. One of the characteristics of the ligand path in classical square-planar d^8 complexes such as Pt(py)$_2$Cl$_2$ is that the second-order rate constant k_Y is strongly dependent on the nature of the incoming ligand. Therefore, the order of nucleophilicity as based on $n°_{Pt}$ values

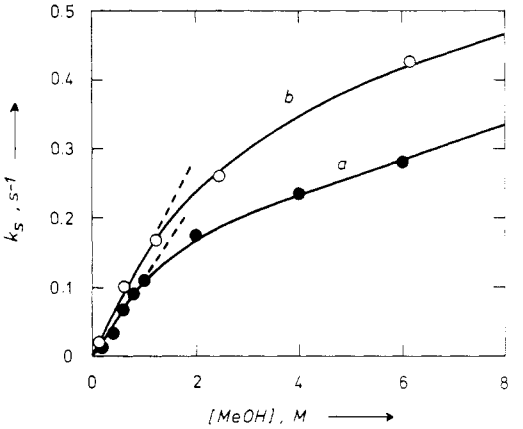

Figure 4. Solvent path for ligand substitution in (a) Ni (SA=*N*-*t*-Bu)$_2$ ([complex] = 2 × 10^{-3} M) and in (b) Cu(SA=*N*-*t*-Bu)$_2$ ([complex] = 1 × 10^{-3} M) by HSA=*N*-Et as a function of increasing concentration of MeOH in toluene at 298 K.

has been set up.[1] It is interesting to see (Table II) that for the ligand substitution in a nickel complex such as Ni(SA=*N*-*t*-Bu)$_2$ the k_{HB} values obtained are also sensitive to the nature of the entering ligands. The following qualitative order is found:

$$\text{HSA=}N\text{-Et} << \text{Hacac} < \text{Hbza} < \text{Hdbm} << \text{Htfa} < \text{Hox} \quad (10)$$

For the ligand HSA=*N*-Et the k_{HB} value is so small that the ligand path is completely covered by the efficient solvent path. The ligand Hox reacts 500 times faster than Hacac. The sharp increase in k_{HB} upon introducing the ligand Htfa instead of Hacac, Hbza, and Hdbm is paralleled by a corresponding sharp increase in the acidity of these ligands (pK_a(Htfa) >> pK_a(Hacac, Hbza, Hdbm) in dioxane/water[17]). The high reactivity of the ligand Htfa is found for the first step of substitution (system 2, k_{HB} = 76.7 M^{-1} s^{-1}) as well as for the second one (k_{HB} = 29.4 M^{-1} s^{-1}). On the basis of acidities only the very poor reactivity of HSA=*N*-Et as well as the very high reactivity of Hox cannot be understood, however.

For a given incoming ligand such as Hacac the comparison of the k_{HB} values for different substrates (systems 5, 9, and 10 in Table II) reveals that the ligand path is 3000–4000 times faster with Ib or Ic than with Ia. Obviously, the Lewis acidity of the substrate as characterized by the equilibrium constants for the addition of pyridine parallels the kinetic findings. In fact, it is the planar ⇌ tetrahedral equilibrium that determines both the Lewis acidity and the kinetic reactivity of these complexes. This parallelism justifies the formulation of a fast preequilibrium (11) in which a 5-coordinate Lewis acid/base adduct between the square-planar conformation of the complex and the incoming ligand is formed.

$$NiA_2 + HB \rightleftharpoons NiA_2 \cdot HB \quad (11)$$

As a matter of fact, in the literature there seems to be general agreement on the mechanism of the ligand path in square-planar d^8 complexes insofar as it is assumed[1] that the rate-determining step is preceded by the association of the incoming ligand.

It appears to be an open question as to which donor atom of the incoming bidentate ligands is coordinated to the nickel in (11). One has to consider, however, that both the complex and the ligands are biphilic in the sense that there are acidic and basic sites in both molecules. As a consequence, a "double acid/base reaction" will take place and lead to the coordination

(17) Van Uitert, L. G.; Fernelius, W. C.; Douglas, B. E. *J. Am. Chem. Soc.* **1953**, *75*, 457.

Scheme II. Mechanism of the Ligand Path

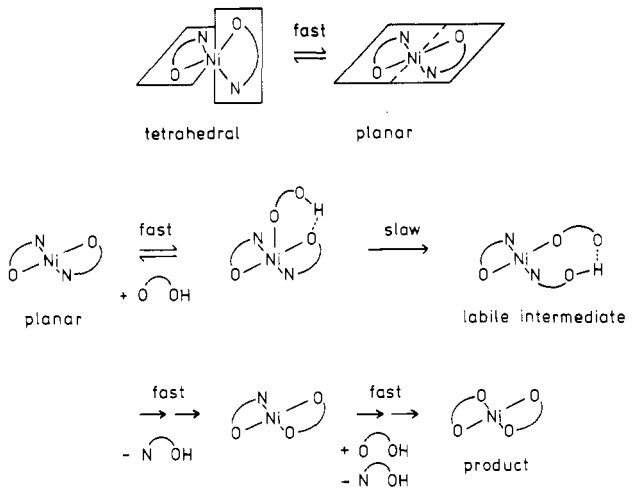

Scheme III. Mechanism of the Solvent Path

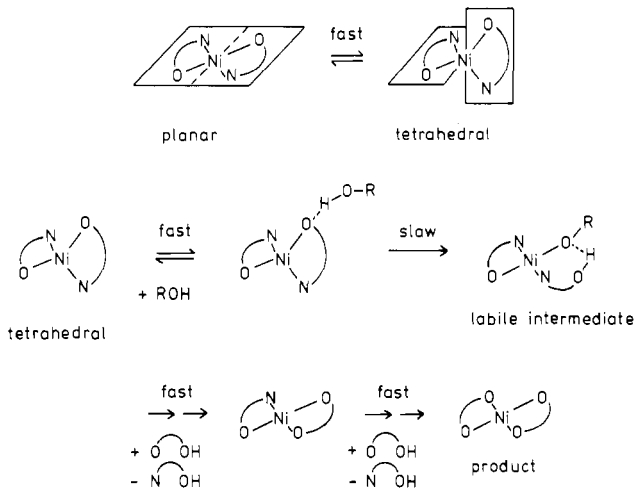

of the bidentate ligand shown in Scheme II. This type of coordination involves hydrogen bonding and implies the formation of 7-membered (HB ≡ Hox) or 8-membered chelate rings.

The extraordinarily high reactivity of Hox in sequence 10 can be explained by the concerted effect of three specific properties: (i) the good donor strength of the pyridine nitrogen, (ii) the relatively high acidity of the phenolic proton, and (iii) the smaller size of the chelate ring formed.

A more detailed description of the mechanism is given in Scheme II (HO̅O and HO̅N are abbreviations for the bidentate ligands involved). All steps following the slow conversion of the 5-coordinate adduct to the labile intermediate seem to be comparatively fast. The only system in which the second step ($NiAB \rightarrow NiB_2$) is slower than the first one ($NiA_2 \rightarrow NiAB$) is system 2 (see Table II).

The data collected in Table II do not provide convincing arguments concerning the effect of the solvent on the ligand path for a given substrate. A comparison of systems 11 and 13 and of systems 7, 12, and 14 reveals only relatively small solvent effects. It is a somewhat puzzling finding, however, that k_{HB}(toluene) < k_{HB}(MeOH) for Ni(SA=*N*-*i*-Pr)$_2$. When pyridine is added to toluene, the rate of ligand substitution in Ni(SA=*N*-*i*-Pr)$_2$ by HSA=*N*-Et through the ligand path drops. This effect is in agreement with the mechanistic interpretation given above: pyridine blocks the axial positions at the nickel and hinders ligand attack according to Scheme II.

Mechanism of the Solvent Path. The discussion of the mechanism of the solvent path has to take into account the following: (i) It is generally assumed for the mechanism of ligand substitution in square-planar platinum complexes that the attack of both the incoming ligand (initiating the ligand path) and the solvent (initiating the solvent path) occurs at the metal. (ii) For the copper complexes Cu(SA=*N*-R)$_2$ studied in methanol the solvent path, as characterized by the size of k_S, decreases with increasing planarity of the complexes (see systems 15–17 in Table II). The data obtained for the corresponding nickel complexes Ia and Ib follow the same sequence, k_S(Ia) > k_S(Ib) (due to a high ligand contribution, k_S(Ic) could be characterized by an upper limit only). (iii) For a given complex the solvent effect has the following order: k_S(MeOH) > k_S(2-PrOH) > k_S(toluene). In fact, in toluene a solvent path was never observed.

The experimental facts summarized in statement ii can be rationalized best by assuming that the tetrahedral conformation of the nickel complexes is involved in the solvent path and that it is induced by solvent attack at the donor oxygen of the coordinated ligands and not at the metal. For an alcohol ROH serving as solvent the attack can be described by Scheme III. Again, all steps following the rate-controlling conversion of the 4-coordinate species Ni(N̅O)$_2$·ROH to the alkoxide intermediate seem to be fast.

The occurrence of mass law retardation in MeOH (see Figure 3a) leads to the postulate that, at least in this solvent, solvolysis[16] according to (12) takes place. In any other alcohol

$$NiA_2(solv) \rightleftharpoons NiA(MeO)(MeOH) + HA \quad (12)$$

ROH applied as solvent the question of whether a neutral nickel species such as NiA(RO)(ROH) + HA or a charged species such as $NiA(ROH)_2^+ + A^-$(solv) is formed will depend on the relative acidities of coordinated HA/ROH and free HA/ROH.

Scheme III is able to explain why k_S is greater for the distorted complex Ia and why k_S does not follow the Lewis acidity of the complexes.

Looking at square-planar and tetrahedral models of the various complexes I, one realizes that the accessibility of the donor oxygen is greater in the tetrahedral than in the planar form. So, the attack of an alcohol molecule ROH according to Scheme III can take place more easily in a distorted complex such as Ia than in a more planar one such as Ib.

It should be pointed out that recently Matsumoto and Kawaguchi[18] have also suggested that the methanol-induced solvent path for ligand substitution in Pd(acac)$_2$ by amines is based on hydrogen bonding between MeOH and the donor oxygen in Pd(acac)$_2$.

Scheme III does not explain the observed occurrence of a solvent path upon addition of pyridine to system 14. A detailed investigation of this phenomenon is in progress.

The fact that the k_S values obtained for Ia and the corresponding copper complex in MeOH (and even in MeOH/toluene mixtures) are very similar would support the interpretation of solvent attack taking place at the coordinated ligand and not at the metal. The activation data for the solvent path, however, are clearly different (see Table III). Assuming similar bond strengths on the basis of similar metal–oxygen bond lengths,[6b] one has to invoke solvation phenomena to explain the differences in $\Delta H^{\ddagger}$ and $\Delta S^{\ddagger}$. It is a matter of fact that the Lewis acidity of the nickel complex is higher than that of the copper complex. It is reasonable to assume therefore that the stronger substrate–solvent interaction in the case of the nickel complex is accompanied by a gain in solvation enthalpy and a loss of entropy. Therefore, $\Delta H^{\ddagger}$(Ni) < $\Delta H^{\ddagger}$(Cu) and $\Delta S^{\ddagger}$(Ni) is much more negative than $\Delta S^{\ddagger}$(Cu). On the basis of Scheme III the sequence k_S(MeOH) >>

(18) Matsumoto, S.; Kawaguchi, S. *Bull. Chem. Soc. Jpn.* **1980**, *53*, 1577.

k_S(2-PrOH) >> k_S(toluene) observed for Ia is in accordance with the ability of the solvents to form hydrogen bonds. For the corresponding copper complex a convincing correlation with Reichardt's solvent polarity parameter $E_T(30)$[19] is obtained for the solvent path in various alcohol solvents.[20]

Scheme III implies that a single alcohol molecule attacks the nickel complex. Since alcohols have to be considered as highly structured liquids, it appeared to be interesting to determine the formal reaction order for the alcohol by diluting it with a kinetically inert cosolvent. Figure 4 presents the data for the system Ia/HSA=*N*-Et/toluene/MeOH. The addition of MeOH to toluene introduces a solvent path, and k_S increases linearly with [MeOH] ≤ 1 M. So, formally k_S is first order in MeOH, which supports Scheme III ($k_S = k_{MeOH}$[MeOH]). Interestingly, the second-order rate constants k_{MeOH} for the corresponding nickel and copper complexes are very similar (see Figure 4; k_{MeOH} = 0.11 M^{-1} s^{-1} for Ia; k_{MeOH} = 0.16 M^{-1} s^{-1} for Cu(SA=*N*-*t*-Bu)$_2$). The decrease in slope at higher methanol concentrations is probably due to the formation of more stable MeOH clusters. The higher reactivity of MeOH at low concentrations appears to be a typical behavior of MeOH admixed to weakly polar cosolvents.[21,22]

(19) Reichardt, C. *Angew. Chem.* **1979**, *91*, 119.
(20) Elias, H.; Wannowius, K. J. *Inorg. Chim. Acta*, in press.
(21) Elias, H.; Gumbel, G.; Neitzel, S.; Volz, H. *Fresenius' Z. Anal. Chem.* **1981**, *306*, 240.
(22) Elias, H.; Muth, H.; Niedernhöfer, B.; Wannowius, K. J. *J. Chem. Soc., Dalton Trans.* **1981**, 1825.

Conclusions

So far a solvent path, although well established for ligand substitution in planar platinum(II) complexes, has not been observed for nickel(II) complexes. The present study provides convincing kinetic data for a first example of 4-coordinate *trans*-N_2O_2 chelate complexes of nickel(II) in which ligand substitution by bidentate entering ligands in alcohol solvents occurs through a solvent path as well as through a ligand-dependent path. It can be demonstrated that the relative contributions of both pathways to the overall rate are governed by the conformational equilibrium planar ⇌ tetrahedral of the substrate and by the type of solvent. There is strong evidence in support of two basically different mechanisms being operative for the two pathways. The ligand-dependent path is induced by ligand attack at the nickel of the planar conformational isomer. The solvent path, however, is initiated by alcohol molecules attacking the tetrahedral conformational isomer at the donor oxygen of the coordinated ligands, most probably through hydrogen bonding.

Acknowledgment. The authors thank the "Deutsche Forschungsgemeinschaft" and the "Verband der Chemischen Industrie e.V." for financial support. Salicylaldehyde was kindly provided by Bayer AG, Leverkusen, Germany.

Registry No. Ia, 40706-02-3; Ib, 35968-67-3; Ib-2py, 35829-39-1; Ic, 35968-61-7; I, R = *n*-Pr-2py, 35829-38-0; I, R = *n*-Bu-2py, 35082-85-0; Ni(5-MeSA=*N*-Et)$_2$, 79898-43-4; Hox, 148-24-3; Htfa, 367-57-7; Hdbm, 120-46-7; Hacac, 123-54-6; HSH=*N*-Et, 5961-36-4; Hbza, 93-91-4; py, 110-86-1; MeOH, 67-56-1; 2-PrOH, 67-63-0.

Contribution from the Istituto della Stereochimica di Coordinazione del CNR, Istituto di Chimica Generale ed Inorganica dell'Università, Florence, Italy, and the Dipartimento di Chimica, Università della Calabria, Cosenza, Italy

Synthesis and X-ray Structure of the Binuclear Complex $[(MeC(CH_2PEt_2)_3)Fe(\mu\text{-}Cl)_3Fe(MeC(CH_2PEt_2)_3)]BPh_4 \cdot CH_2Cl_2$. Interpretation of the Geometrical and Electronic Features through a Recent MO Approach for M_2L_9 Complexes

C. BIANCHINI,[1a] P. DAPPORTO,[1b] C. MEALLI,*[1a] and A. MELI[1a]

Received April 23, 1981

A stable tri-μ-chloro binuclear complex of iron(II) can be formed with the tripod ligand 1,1,1-tris((diethylphosphino)-methyl)ethane (etriphos). The X-ray structure determination of the compound $[Fe_2Cl_3(etriphos)_2]BPh_4 \cdot CH_2Cl_2$ (triclinic $P\bar{1}$, a = 18.835 (6) Å, b = 17.433 (6) Å, c = 10.977 (4) Å, α = 106.65 (5)°, β = 92.52 (5)°, γ = 107.24 (5)°) has shown that the geometry is confacial bioctahedral. With use of the Summerville and Hoffmann recent theoretical approach to M_2L_9 complexes, a comparison of the geometrical and electronic features of this complex with those of the analogous $[Fe_2H_3(triphos)_2]PF_6 \cdot 1.5CH_2Cl_2$ (triphos = 1,1,1-tris((diphenylphosphino)methyl)ethane) is performed. A particularly good agreement is observed between the elongation of the bioctahedron experimentally observed in this tri-μ-chloro complex and that predicted by MO calculations for the $[Fe_2Cl_3(CO)_6]^+$ model.

Introduction

Recently Summerville and Hoffmann have studied in detail the MO structure of confacial bioctahedral complexes of the type $L_3MX_3ML_3$.[2] A number of molecular models with either π-acceptor or -donor terminal ligands and hydride, chloride, and carbonyl as representative bridging ligands were investigated. The theoretical results for tri-μ-hydrido species were compared with the geometrical details of the few existing structures, two of which were previously characterized in this laboratory,[3] namely, $[Fe_2H_3(triphos)_2]PF_6 \cdot 1.5CH_2Cl_2$ (**1**) (triphos = 1,1,1-tris((diphenylphosphino)methyl)ethane) and $[Co_2H_3(as_3)_2]BPh_4$, **2**, (as_3 = 1,1,1-tris((diphenylarsino)-methyl)ethane). Calculations were also performed for tri-μ-chloro species by using the model $[Fe_2Cl_3(CO)_6]^+$. The symmetry-conditioned opportunities for interactions between the metals and the bridging groups orbitals as well as direct metal–metal interaction are quite different in the two cases. X-ray structures of confacial bioctahedral complexes with three bridging chlorine atoms and terminal π-acceptor ligands are limited to the $[Ru_2Cl_3(CO)_5SnCl_3]$ complex.[4] Otherwise one has to refer to complexes with π-donor bridging groups of different nature such as mercapto groups.[5,6] The effect of

(1) (a) Istituto della Stereochimica di Coordinazione del CNR. (b) Università della Calabria.
(2) Summerville, R. H.; Hoffmann, R. *J. Am. Chem. Soc.* **1979**, *101*, 3821.
(3) Dapporto, P.; Midollini, S.; Sacconi, L. *Inorg. Chem.* **1975**, *14*, 1643.
(4) (a) Pomeroy, R. K.; Elder, M.; Hall, D.; Graham, W. A. G. *Chem. Commun.* **1969**, 381. (b) Elder, M.; Hall, D. *J. Chem. Soc. A* **1970**, 245.
(5) Shultz, A. J.; Eisenberg, R. *Inorg. Chem.* **1973**, *12*, 518.

0020-1669/82/1321-0612$01.25/0